 doi:10.20944/preprints202105.0577.v1

Research Article

Fatty acid and proteomic signatures of circulating CD81 positive small extracellular vesicles define the disease stage in melanoma patients

Giovanni Paolino[1,2]†, Veronica Huber[3]†, Serena Camerini[4], Marialuisa Casella[4], Alberto Macone[5], Lucia Bertuccini[6], Francesca Iosi[6], Elisa Moliterni[1], Serena Cecchetti[7], Irene Ruspantini[4], Flavia Chiarotti[8], Carla Raggi[9], Antonella Di Biase[10], Stefano Calvieri[1], Santo Raffaele Mercuri[2], Luana Lugini[11]‡, Cristina Federici[11]‡.

[1] Department of Dermatology, Sapienza University of Rome, Italy.

[2] Unit of Dermatology and Cosmetology, IRCCS University Vita-Salute San Raffaele, Milan, Italy.

[3] Unit of Immunotherapy oh human tumors, National Institute of Tumors, Milan, Italy.

[4] Core Facilities Mass Spec Unit, National Institute of Health, Rome, Italy.

[5] Department of Biochemical Sciences "A. Rossi Fanelli", Faculty of Pharmacy and Medicine, Sapienza University of Rome, Italy.

[6] Core Facilities Electron Microscopy Unit, National Institute of Health, Rome, Italy.

[7] Core Facilities Unit Confocal Microscopy, National Institute of Health, Rome, Italy.

[8] Reference Center for Behavioral Sciences and Mental Health, National Institute of Health, Rome, Italy.

[9] National Centre for the Control and Evaluation of Medicines, National Institute of Health, Rome, Italy.

[10] Department of Food Safety, Nutrition and Veterinary Public Health, National Institute of Health, Rome, Italy.

[11] Department of Oncology and Molecular Medicine, National Institute of Health, Rome, Italy.

†These authors have contributed equally to this work.

‡LL and CF are co-last and co-corresponding authors.

Correspondence: LL email: luana.lugini@iss.it ; CF email: cristina.federici@iss.it ; Tel.: +390649902879

 doi:10.20944/preprints202105.0577.v1

Simple Summary:

The early detection of cutaneous melanoma is key to increase survival and therapeutic adjustment and especially in stages II-IV biomarkers are urgently needed. We investigated if fatty acid (FA) and protein composition of small extracellular vesicles (sEV) deriving from plasma of 0-I, II, and III-IV stage melanoma patients could reflect disease stage and thus function as biomarker. Results showed a higher content of FA and a decrease in Saturation Index (C18:0/C18:1), already detectable in early stages, that distinguished patients' CD81sEV from HD. Proteomics (identifier PXD024434) detected an exclusive increase of CD14, PON1, PON3 and APOA5 in stage II and a decrease of Rap1b in stage III-IV CD81sEV. This stage dependent sEV signature strengthens the potential of sEV in providing discriminatory information for early diagnosis, prediction of metastatic behavior, treatment and follow up of melanoma patients.

Abstract:

The early detection of cutaneous melanoma, a potentially lethal cancer with rising incidence, is key to increase survival and therapeutic adjustment. Especially in stages II-IV biomarkers are urgently needed for adjuvant therapy purposes after resection and for treatment of metastatic patients. We here investigated if fatty acid (FA) and protein composition of small extracellular vesicles (sEV) deriving from plasma of 0-I, II, and III-IV stage melanoma patients (n=38) could reflect disease stage and thus function as biomarker. The subpopulation of sEV expressing CD81 (CD81sEV) was isolated by an ad hoc immune affinity technique from microvesicle-depleted plasma. Biological macromolecules were investigated by gas chromatography and mass spectrometry in CD81sEV. A higher content of FA and a decrease in Saturation Index (C18:0/C18:1), already detectable in early stages, distinguished patients' from healthy donor CD81sEV. Proteomics (identifier PXD024434) detected an exclusive and significant increase of CD14, PON1, PON3 and APOA5 in stage II and a significant decrease of Rap1b in stage III-IV CD81sEV. The FA and proteomic stage dependent CD81sEV signature strengthens the potential of circulating sEV studies in providing discriminatory information for early diagnosis, prediction of metastatic behavior and follow up of melanoma patients.

Keywords: Melanoma patients; Small Extracellular Vesicles; Proteomics; Fatty acids; Biomarkers

Preprints (www.preprints.org) | NOT PEER-REVIEWED | Posted: 24 May 2021 doi:10.20944/preprints202105.0577.v1

1. Introduction

Extracellular vesicles (EV) characteristics change depending on the status of the releasing cells. Cancer impacts the host's body at different levels and circulating EV may reflect the actual disease status [1]. Thus, EV monitoring represents a promising non-invasive strategy to obtain biomarkers of diagnosis, progression, response or resistance to therapy [2, 3]. EV comprise different subfamilies including exosomes, lipid bilayer-surrounded endosomal-derived vesicles of 30-150 nm. The identification of biomarkers of early detection and prediction of recurrence risk has demonstrated the feasibility of subtyping breast cancer by proteomic analysis of serum EV [4]. Additionally, the integrin landscape of tumor EV allows anticipating the metastatic behavior [5]. Melanoma EV foster progression, immune suppression, epithelial-to-mesenchymal transition, promote the establishment of premetastatic niche and counter anti-cancer therapies [6]. At difference to healthy donors (HD), plasma of melanoma patients contains higher amounts of EV exposing melanoma inhibitory activity (MIA) and calcium binding protein B (S100B), together with CD63 and Caveolin-1 [7, 8]. Cutaneous melanoma is an aggressive cancer that tends to early metastasis and with a worldwide increasing incidence. In advanced stages, despite the advent of targeted and immunotherapies, the prognosis remains generally poor due to tumor immune escape and intrinsic cell resistance [9-11]. Surgery is the treatment of choice in early stages, while advanced stages require systemic therapy [12]. Tumor thickness, ulceration, invasion of blood vessels or lymphatics and immune response are the predominant tools to determine prognosis [13]. Tumor, nodes, metastasis (TNM) classification and stage grouping criteria facilitate accurate risk stratification to guide patient treatment [14].. Early detection of melanoma and its metastases play a key role in increasing survival and therapeutic adjustment. The lack of specific biomarkers encourages the identification of new candidates, especially in stages II-IV, for adjuvant therapy purposes after resection, as well as for therapies in metastatic patients. Several molecules were proposed as prognostic markers: S100B, MIA, LDH, and BRAF mutation [15, 16]. Cell-free nucleic acids and circulating tumor cells, detectable in 29–72% metastatic patients, are prognostic for overall survival [17]. Additionally, PD-L1 immune checkpoint, exposed by tumor and non-tumor EV, has been tested as response biomarker of immunotherapy with PD-1 checkpoint inhibitors [18]. In contrast, studies quantifying lipid species in cancer patients' body fluid EV are only starting to emerge, as shown for prostate cancer [19]. Exosomes are enriched in sphingolipids, cholesterol, phosphatidylserine and display a higher saturation level of the fatty acyl groups in phospholipids, with respect to their originating cells. Their composition is similar to lipid rafts, and exosomes have a higher lipid order and detergent stability than other EV types [20]. Exosomal lipid profiles may also reflect their phenotype and functions [21, 22].

Here we combined fatty acids (FA) and proteomic studies to investigate potential differences of plasma small EV (sEV) profiles of different stage (0-IV) melanoma patients and compared them to HD. In particular, we focused on immunoaffinity-captured $CD81^+$ sEV (CD81sEV) to investigate potential discriminatory information for early stage melanoma patients that contributes to early diagnosis and predicts metastatic properties. We also aim at understanding if proteome and FA signatures of circulating melanoma patients' CD81sEV can reflect the alterations induced by the tumor at liquid biopsy level.

2. Materials and Methods

2.1 Human subjects

Blood was obtained from fasting melanoma patients (n=38), stages 0-IV (Table S1), and from age and gender matched healthy donors (HD=17) routinely donating blood at Centro Trasfusionale Universitario of Azienda Policlinico Umberto I, Sapienza University of Rome, Italy. Subjects signed informed consent approved by Centro Trasfusionale Universitario and Clinica Dermatologica of Azienda Policlinico Umberto I, Sapienza University of Rome, Italy (Board resolution approval number #35/2017). Heparinized blood was diluted 1:2 with PBS1X, centrifuged at 1,200 x g for 20 min and plasma was collected and stored at -80°C.

2.2 Total sEV isolation

sEV were isolated as described, with modifications [23]. Briefly, the plasma was centrifuged for 30 min at 500 × g and 45 min at 12,000 × g (to discard microvesicles), 0.45-µm filtered (Sartorius, Germany), and ultracentrifuged for 2 h at 110,000 × g at 10°C (Sorvall WX Ultra Series centrifuge, F50L-2461.5 rotor, Thermo Scientific, Germany). The pellet was suspended in PBS, ultracentrifuged at 110,000 × g for 90 min and preserved for subsequent analyses.

Preprints (www.preprints.org) | NOT PEER-REVIEWED | Posted: 24 May 2021 doi:10.20944/preprints202105.0577.v1

2.3 Immunocapture of CD81sEV

To investigate a homogeneous EV population and exclude lipoprotein contamination we captured sEV expressing CD81 pan EV marker. Protein A+G Sepharose resin (Pierce, Thermo Fisher Scientific) was washed twice with sodium tetraborate 0.1 M pH 9.0 and incubated with monoclonal anti-CD81 antibody (B-11, Santa Cruz Biotechnologys Heidelberg, Germany) in rotation at RT. After washes, the resin was resuspended in 0.1M sodium tetraborate containing 20 mM dimethyl pimelimidate DMP (Pierce) crosslinker and incubated o.n. After washing twice with 50 mM Tris pH 7.5 the resin was incubated o.n. with plasma, previously diluted 1:1 and centrifuged for 45 min at 12,000 × g, to capture CD81sEV.

2.4 Electron Microscopy

Transmission (TEM), scanning (SEM) and immune electron microscopy were performed on sEV purified from 2 ml of plasma [23, 24]. CD81 and TSG101 were detected using B11 monoclonal antibody (Santa Cruz) and polyclonal anti-tsg101 antibody (ab70974, Abcam, Cambridge, United Kindom). Grids were observed by PHILIPS EM208S transmission electron microscope (FEI - Thermo Fisher Scientific, Germany).

2.5 Nanoparticle tracking analysis of sEV

Total sEV were subjected to nanoparticle tracking analysis (NTA, NanoSight NS300, Malvern Panalytical, UK). Detection conditions: capture level 15, threshold 5, slider gain 366, capture duration 60 s. Five videos of 60 s were recorded and analyzed by NTA 3.0 software (Malvern Instruments).

2.6 FA Gas Chromatography of total sEV

Lipids were transmethylated with Boron trifluoride-methanol solution (Sigma-Aldrich) at 70°C. Fatty acid methyl esters (FAME) were extracted and analyzed by gas chromatography (Agilent, Palo Alto, CA), equipped with a fused silica capillary column (Omegawax 250, 30m x 0.25mm i.d. and 0.25 μm film thickness, Supelco, Sigma-Aldrich) and a flame ionization detector. The injector (split 5:1) temperature was 260°C, and the detector temperature was set at 280°C. The heating program began at 190°C, increased by 2°C per minute and was held at 240°C. FAME were identified by comparison with authentic standards (Supelco) and calculated as percentages of total FA. Data were analyzed by Prism (Graphpad).

2.7 FA GC-MS analysis of CD81sEV

Membrane phospholipids were extracted and transmethylated [25]. Fatty acid methyl esters were measured with an Agilent 7890B gas chromatograph coupled to a 5977B quadrupole mass selective detector (Agilent Technologies, Palo Alto, CA). Separations were carried out with an Agilent HP5ms fused-silica capillary column (30m × 0.25mm i.d.) coated with 5%-phenyl-95%-dimethylpolysiloxane (film thickness 0.25 μm) as stationary phase. Injection mode: splitless at a temperature of 280 °C. Column temperature program: 120 °C (1 min) then to 320 °C at a rate of 20 °C/min and held for 10 min. The carrier gas was helium at a constant flow of 1.0 ml/min. The spectra were obtained in the electron impact mode at 70 eV ionization energy; ion source 280 °C; ion source vacuum 10-5 Torr. MS analysis was performed simultaneously in TIC (mass range scan from m/z 50 to 600 at a rate of 0.42 scans s-1) and SIM mode. Data were analyzed by Prism (Graphpad).

2.8 LC-MS/MS proteomics of CD81sEV

Electrophoresis was performed on NuPAGE 4–12% (Novex, Invitrogen, CA), loading 8 μg for each CD81sEV deriving from a pool of 2 melanoma patients or 2 HD. For each stage, (0-I, II, III-IV) and HD we analyzed 3 pools, for a total of 6 samples/group. Each gel lane was almost completely cut in 10 slices, avoiding only areas close to 50 and 25 KDa to elude IgG and serum albumin contaminants. Coomassie (Colloidal Blue Staining kit, Invitrogen) stained proteins were enzymatically *in gel* digested after reduction and alkylation of cysteine residues [26]. The peptide mixture was desalted on a trap column (Acclaim PepMap 100 C18, Thermo Fisher Scientific) and separated on a 20-cm-long silica capillary (Silica Tips FS 360-75-8, New Objective), packed in-house through a reverse-phased capillary high pressure liquid chromatography using an UHPLC nano system (Ultimate 3000 Dionex, Thermo Fisher Scientific), with a 75 min long acetonitrile gradient with a flow rate of 250 nl/min [23]. Eluted peptides were in-line introduced to an Orbitrap Fusion Tribrid Mass Spectrometer (Thermo Fisher Scientific, CA). Orbitrap detection was used for MS1 measurements, at resolution of 60 K (at m/z 200), while MS2 was performed in the ion trap with a rapid scan rate. The most abundant quadrupole isolated precursors were selected in the range of m/z 350-1550 and a data-dependent MS/MS analysis was performed in top speed mode with a 3 s cycle time. Precursors were fragmented with HCD using 32% of normalized collision energy and dynamic exclusion was enabled for 60 s. A standard Automatic Gain Control (AGC) with 50 ms of

Preprints (www.preprints.org) | NOT PEER-REVIEWED | Posted: 24 May 2021 doi:10.20944/preprints202105.0577.v1

maximum injection time was used for MS1, while 20% of normalized custom AGC with a dynamic maximum injection time mode was applied for MS2.

2.9 Computational MS data analysis of CD81sEV

MS raw files were analyzed by Proteome Discoverer 2.4 software (Thermo Fisher Scientific) and peak lists were searched against the human database from UniProtKB/Swiss-Prot database (Release 25 October 2017; 42253 sequences) by Sequest HT search engine. Peptide identification was obtained using the precursor and fragment tolerance of 10 ppm and 0.6 Da, respectively. Cysteine carbamidomethylation was used as fixed modification while methionine oxidation and N-acetylation on protein terminus were set as variable modifications; specific trypsin cleavage with two miscleavages were allowed. False discovery rate was set to 1% and determined by searching a reverse database using Percolator node, based on q values. Label-free quantification was based on precursor intensity using all peptides. The proteins were analyzed by VENN diagram (http://bioinformatics.psb.ugent.be/webtools/Venn/). Enrichment analyses including comparison with Vesiclepedia and Exocarta database (http://www.exocarta.org/) [27] were performed using FunRich 3.1.3 [28, 29] http://www.funrich.org. Protein-protein interaction was analyzed by String v 11.0 (https://string-db.org/) [30]. MS data were deposited to the ProteomeXchange Consortium via the PRIDE [31] partner repository, dataset identifier PXD024434".

Proteins were analyzed following the 'DEP package' [32] within the Bioconductor project [33] and based on the statistical programming language R. After quantification, data underwent: 1) filtering: proteins (n=526) were selected when showing at least the 80% of valid values; 2) variance stabilizing transformation for normalization; 3) imputation according to 'minDet' method replacing the missing entries with an estimated minimal value observed in each sample. To identify differentially expressed proteins, the three stages were compared to HD, by combined approach relying on protein-wise linear models and empirical Bayes statistics [34]. Proteins were marked as significant based on two thresholds: a p-adjusted lower than 0.05 and a fold change higher than 1.5. Correction was applied for multiple hypotheses testing through the algorithm of false discovery rate estimation as implemented in the 'fdrtool' package [35].

3. Results

3.1 Total sEV of melanoma patients and HD

Our principal aim was to verify if in early stages including stage 0-I (in situ melanoma) and stage II we could detect discriminating characteristics with respect to stage III-IV advanced patients and in comparison to HD. We isolated total sEV by differential centrifugation and our protocol included a 45 min 12,000 x g step followed by 0.45 μm filtration to eliminate microvesicles. SEM (Figure 1A, panels a and b) and TEM (Figure 1A, panels c and d) showed the presence of vesicles displaying the typical structure and dimensions of exosomes, as depicted for representative HD and melanoma stage II sEV. The expression of CD81 and TSG101 proteins confirmed their exosomal-like nature (Figure 1A, panels e and f HD; g and h patient; CD81 and TSG101, respectively). NTA profiling highlighted differences in particle concentration and size (mode and mean), as shown by the representative spectra of a HD and different stage patients (Figure 1B). Of note, the number of circulating sEV augmented with progression and differences between stage 0-I and stage II and stage III-IV were statistically significant (Figure 1C). NTA also revealed that circulating sEV of patients were smaller (mean 93.8+/-9.4; mode 67.2 +/-8.2) than those of HD (mean 107.7 +/-10; mode 83.8+/-8.0) and this difference was maintained throughout the stages (Figure 1C).

Preprints (www.preprints.org) | NOT PEER-REVIEWED | Posted: 24 May 2021 doi:10.20944/preprints202105.0577.v1

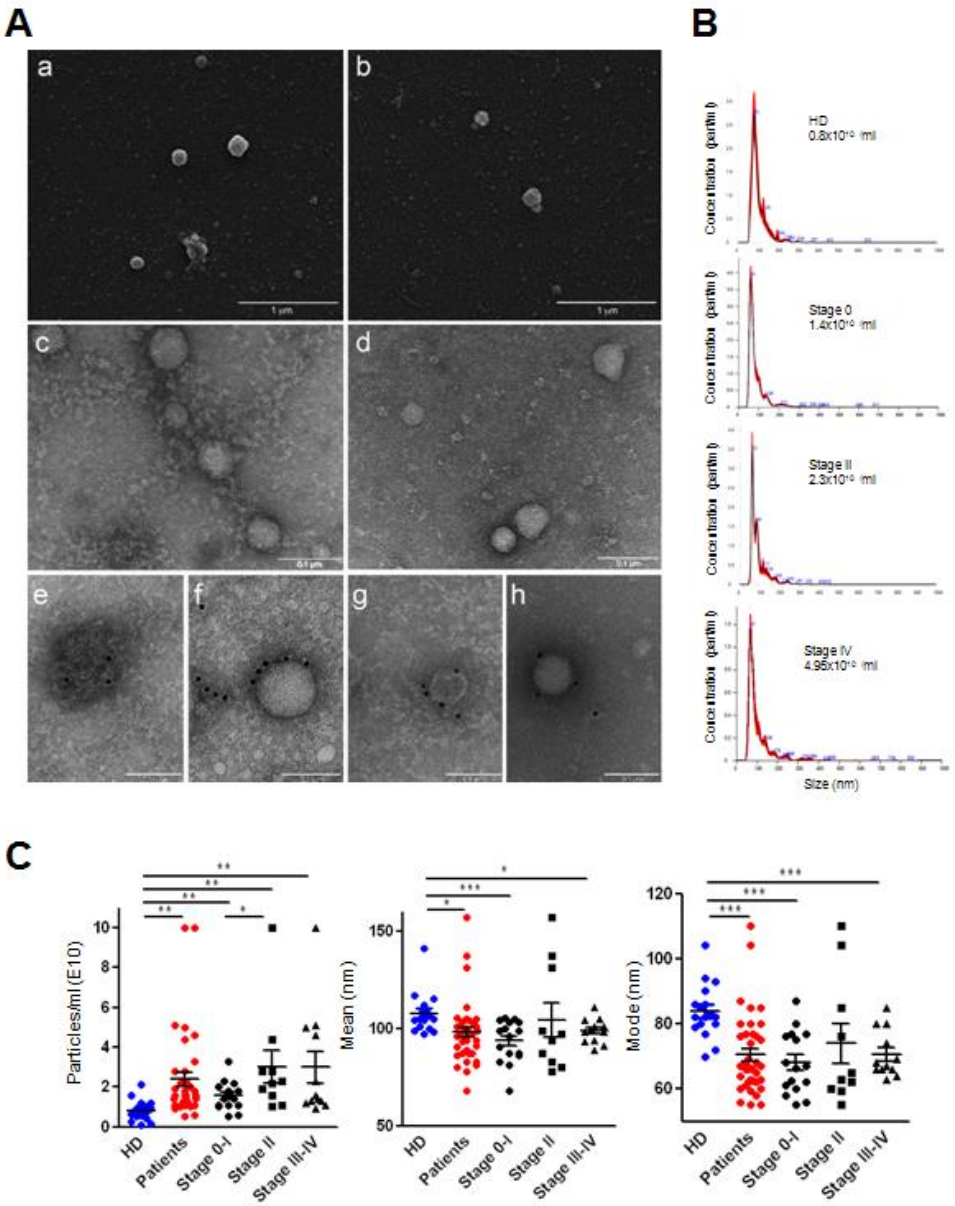

Figure 1. sEV morphology and Nanoparticle tracking analysis (NTA). A. Scanning electron microscopy analysis of sEV from a HD (a), and from a stage II melanoma patient (b), bars, 1 µm; Transmission electron microscopy analysis of HD sEV (c) and stage II patient's sEV (d), bars, 0.1 µm; (E-H): Immunoelectron microscopy combined with positive/negative contrast method of a HD sEV (e, f) and a stage II patient's sEV (g, h) revealed the presence of CD81 (e, g) and TSG101 (f, h), bars, 0.1 µm. **B.** Representative NTA profiles HD and melanoma patients (stage 0, II, IV) sEV. C, NTA characterization of sEV from HD and patients, in different stages of disease (particles/ml, mean and mode), HD n=17, patients n=38. Statistical significance was achieved with unpaired t-test. * $p<0.05$, ** $p<0.001$, *** $p<0.0001$.

3.2 FA signature in total and CD81sEV

GC FA analysis of total sEV showed a prevalence of saturated FA, essentially palmitic (C16:0) and stearic acids (C18:0) (Figure 2A). Compared to HD, patient sEV showed a decrease of saturated FA (C16:0, C18:0, C20:0, C22:0) and the increase of unsaturated FA (C18:1, C18:2n6, C20:4n6). These differences were maintained throughout the stages 0-I, II, III-IV (Figure S1). The saturation index (SI=C18:0/C18:1) (36) of sEV evidenced a decrease in patients' sEV (Figure 2B). Capturing CD81sEV led to the loss of long/very long chain FA and evidenced differences in FA profiles. In contrast to total sEV the interstage differences became evident in CD81sEV. Patients displayed a higher content of FA compared to HD, particularly evident for C12 lauric, C14 myristic, C16 palmitic, C18 stearic and C18:1 oleic acids (Figure 2C). The SI (18:0/18:1) of CD81sEV revealed a strong reduction in stage II and III-IV patients (Figure 2D). The single FA in CD81sEV revealed the expression of C12:0 and C14:0 FA at high level in advanced stages, although these FA are usu-

Preprints (www.preprints.org) | NOT PEER-REVIEWED | Posted: 24 May 2021 doi:10.20944/preprints202105.0577.v1

ally expressed at very low level in human cells. Moreover, C18:0 and C18:1 levels were significantly different between early and late stages and even more in comparison to HD (Figure 2E).

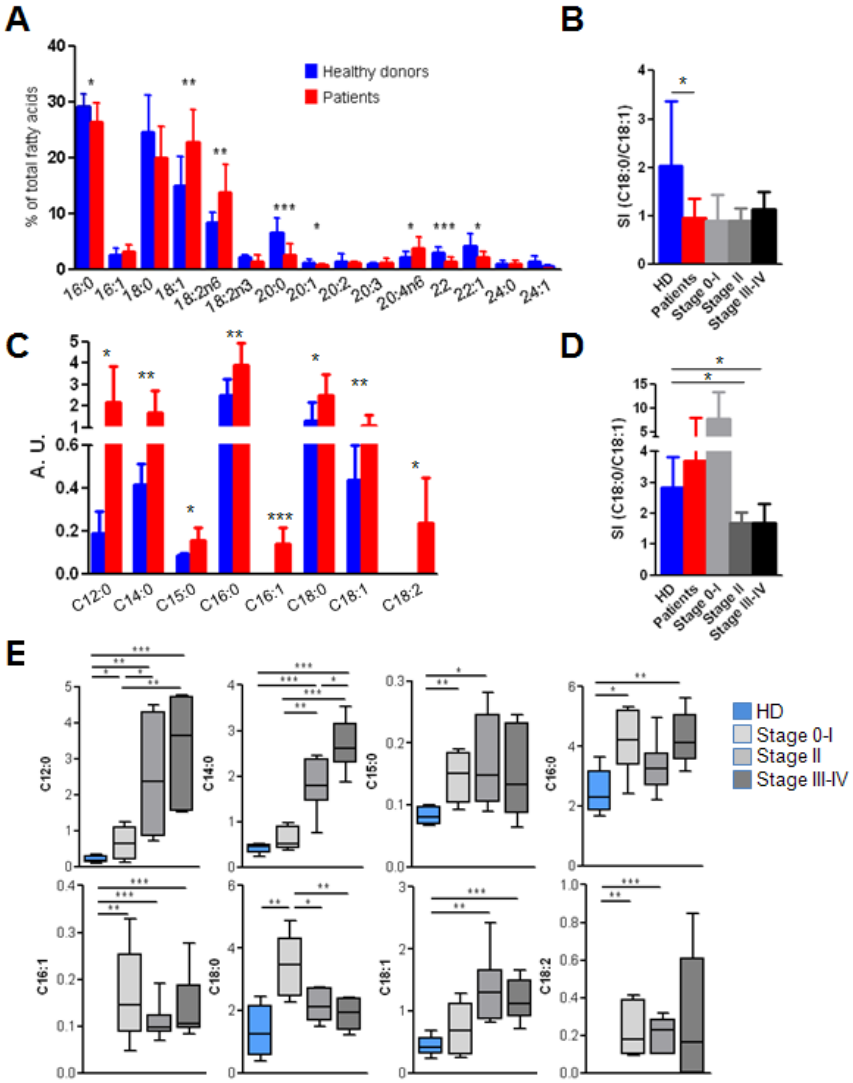

Figure 2. Fatty acids in total sEV and CD81sEV. A. Analysis by Gas Chromatography of FA in total sEV from HD and melanoma patients. B. Saturation Index (SI=C18:0/C18:1) of the samples in A.; C. Gas Chromatography and Mass Spectrometry analysis of FA in CD81-immunocaptured sEV from HD and patients; D. the respective SI of the samples in C. E. Single FA of stage 0-I, II and III-IV vs HD in CD81sEV. Statistical significance was achieved with unpaired t-test. * $p<0.05$, ** $p<0.001$, *** $p<0.0001$.

3.3 Proteomic analysis of CD81sEV

CD81sEV of 0-I, II and III-IV stages and HD were analyzed by LC-MS/MS. We identified a total of 899 proteins quantifying 826 of them (Proteome Xchange with identifier PXD024434). We found small differences among the proteins detected in each biological replicate (Supplementary Figure S2A), with an average of 631 proteins detected in each sample (Supplementary Figure S2B). The biggest portion (average 87%) of proteins was detected at least in two independent samples (Figure S2C and D). Venn diagram (Figure 3A) showed a small number (56 corresponding to 7% of the total) of proteins uniquely detected in each sample (healthy or melanoma stage) and almost all of these were identified only one time, indicating that these were likely low abundant and thus close to the sensitivity threshold or specific to single samples. Only 6 proteins were identified at least two times uniquely in specific samples and comprised Filamin B for HD, Integral membrane protein 2B and Palmitoyl-protein thioesterase 1 for stage 0-I, Insulin-like growth factor-binding protein 5 and Syntenin-1 for stage II and Dyslexia-associated protein KIAA0319-like protein for stage III-IV (Figure 3, Table B). Comparison with Vesiclepedia using the FunRich tool evidenced 97% of the proteins detected in our samples were present in the database comprehensive of all vesicle types and 95% in that specific for ex-

Preprints (www.preprints.org) | NOT PEER-REVIEWED | Posted: 24 May 2021 doi:10.20944/preprints202105.0577.v1

osomes (Supplementary Figure 3E, F). Moreover, 81% of the top 100 Vesciclepedia proteins were detected in our dataset (Supplementary Figure 3G). Similarly, the comparison with Exocarta database evidenced 83% of proteins as common (Supplementary Figure 3H). Cellular component analysis also showed the highest enrichment in exosomes (Figure 3C), confirming the good quality of our preparations. The comparison with the FunRich database of site of protein expression showed a significant enrichment of our protein set in melanoma and in immune cells, including neutrophils, monocytes, B cells and CD4 and CD8 T cells (Figure 3D). The analysis of the biological processes involving the detected proteins showed a significant enrichment particularly in protein metabolism, cell growth and/or maintenance and immune response (Figure 3E).

A

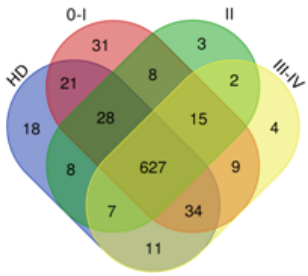

B

Sample	Accession	Description	n° detections
HD	O75369-1	Filamin-B	2
Stage 0-I	Q9Y287	Integral membrane protein 2B	3
Stage 0-I	P50897	Palmitoyl-protein thioesterase 1	2
Stage II	P24593	Insulin-like growth factor-binding protein 5	2
Stage II	O00560-1	Syntenin-1	2
Stage III-IV	Q8IZA0	Dyslexia-associated protein KIAA0319-like protein	2

C

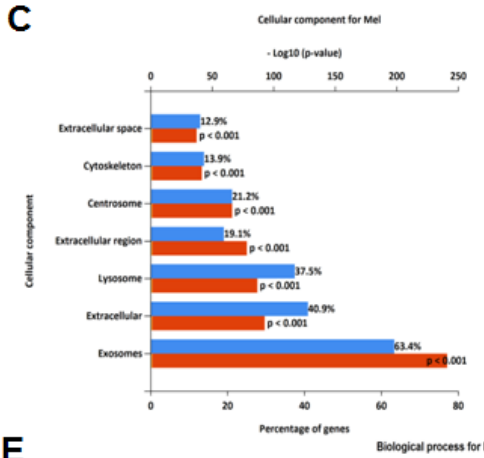

D

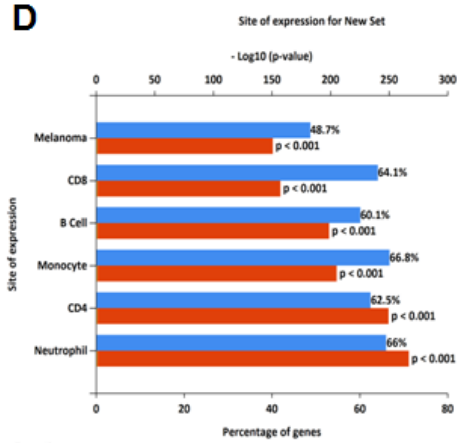

E

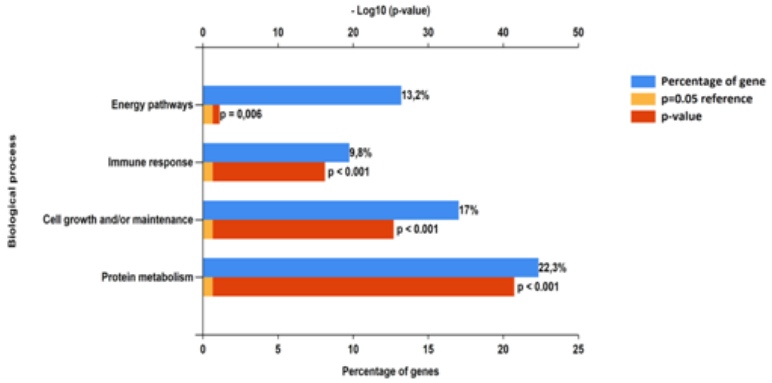

Figure 3. Proteomic analysis of CD81sEV by Mass Spectrometry. A. Venn diagram representing the number of proteins uniquely detected or shared with other samples in each HD, stage 0-I, stage II, stage III-IV group. B. Table of proteins identified at least two times specifically in one sample group. C. Enrichment analysis of identified proteins by FunRich analysis for cellular component, site of expression (D), and biological process (E). Blue bars represent the percentage of protein genes assigned to the indicated term, yellow bars show the reference p value (0.05), and red bars show the calculated p value of enrichment for the indicated term.

Preprints (www.preprints.org) | NOT PEER-REVIEWED | Posted: 24 May 2021 doi:10.20944/preprints202105.0577.v1

The proteins detected by mass spectrometry were also quantified by label free approach. Five proteins were found as significantly differentially expressed (Figure 4A): the proteins APOA5, PON1, PON3 and CD14 were increased in stage II CD81sEV in comparison with HD (Figure 4B), while the protein Rap-1b decreased in stage III-IV patients vs HD. We detected the highest difference between HD and stage II, with respect to the other pairs. Protein-protein interaction among was analyzed by STRING (Figure 4C) and three proteins (PON3, PON1, and APOA5) had direct interactions and two biological processes were enriched (FDR<0.05): PON1 and PON3 are involved in the lipoxygenase pathway while APOA5, Rap-1b and CD14 are involved in the regulation of vesicle-mediated transport.

A

Change	Accession	Gene Symbol	Protein description
Up in II *vs* HD	Q6Q788	APOA5	Apolipoprotein A-V
Up in II *vs* HD	P27169	PON1	Serum paraoxonase/arylesterase 1
Up in II *vs* HD	Q15166	PON3	Serum paraoxonase/lactonase 3
Up in II *vs* HD	P08571	CD14	Monocyte differentiation antigen
Down in III-IV *vs* HD	P61224-1	RAP1B	Ras-related protein Rap-1b

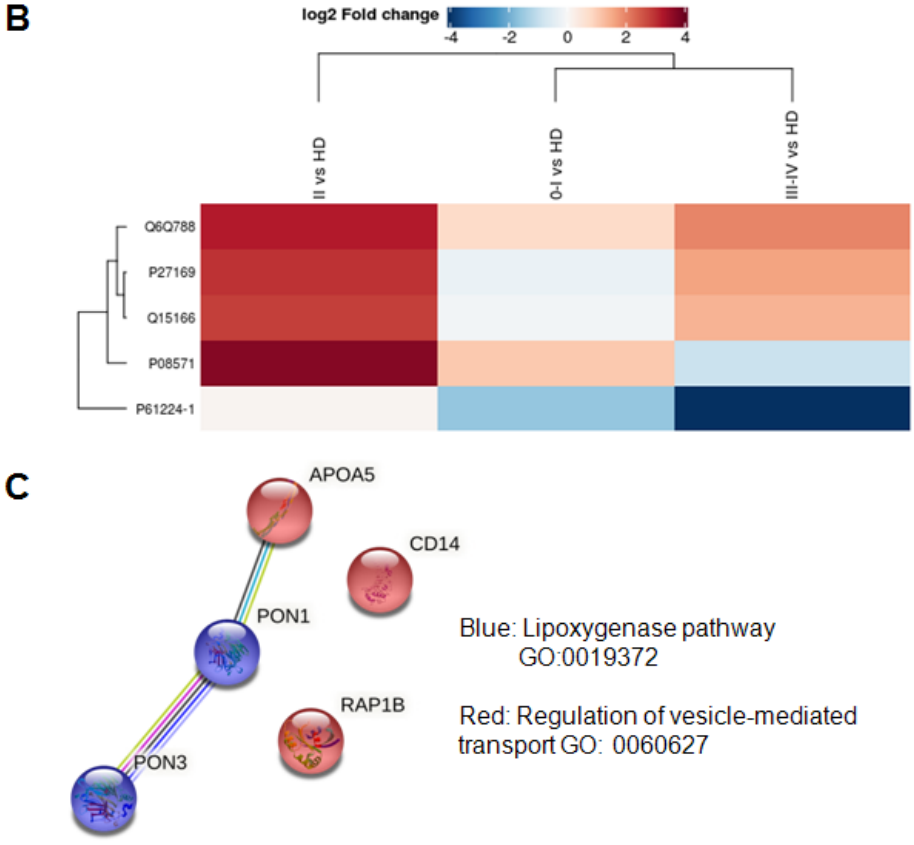

Figure 4. **Analysis of differently expressed proteins in CD81sEV**. A. Table of proteins found as statistically differently expressed in sEV from HD versus patients. B. Protein fold change in the different stages. The proteins APOA5 (Q6Q788), PON1 (P27169), PON3 (Q15166), CD14 (P08571) increased in the stage II in comparison with HD, while protein Rap-1b (P61224-1) decreased in the stage III-IV versus HD. C. Protein-protein interaction among proteins analyzed by STRING. Blue circles belong to Lipoxygenase pathway (GO:0019372), red circles to the Regulation of vesicle-mediated transport (GO: 0060627).

 doi:10.20944/preprints202105.0577.v1

4. Discussion

Despite representing less than 5% of all cutaneous malignancies, melanoma accounts for the majority of skin cancer deaths [37]. Although the advent of targeted and immune therapies have improved the median survival for metastatic patients, biomarkers of surveillance and early detection of initiation and progression are urgently needed to guide clinical intervention. In this context, the protein content of sEV isolated from plasma may be informative [38]. Lipid metabolic alterations in tumor cells have attracted major interest [39], as they are essential for progression and aggressiveness. We and others have previously found that advanced melanoma patients have increased amounts of circulating EV compared to HD [8], the protein amount is higher in late versus early stages and decreases in response to therapy [40]. Here we show that increased sEV concentrations are detectable already in stages 0-II (Figure 1C) and sEV showed a 20% size reduction. Such characteristics may facilitate EV distribution to lungs and crossing the blood-brain barrier, promoting pre-metastatic niche formation [41]. On the other hand we cannot rule out that the increase in concentration of sEV, isolated as bulk sEV by ultracentrifugations, might derive from lipoproteins precipitating during the ultracentrifugation step despite our sEV isolation protocol included a 12,000 x g centrifugation of 45 min to reduce such contaminations [42]. Similarly, bulk sEV contained long and very long-chain FA that were not detectable in CD81sEV potentially deriving from lipoprotein contaminants precipitating during EV isolation (Figure 2A, B) [42, 43]. FA analysis of CD81sEV revealed a higher content of the FA C12 lauric, C14 myristic, C16 palmitic, C18 stearic and C18:1 oleic acids (Figure 2C). The SI (18:0/18:1) decerased in stage II and III-IV patients, suggesting a link with disease progression (Figure 2D). The SI was proposed as malignancy marker, consistently with the reduced SI in neoplastic cells and in red blood cell (rbc) membranes of cancer patients [36, 44]. In fact, FA analysis of rbc membranes from cancer patients presented a lower relative percentage of saturated FA, higher levels of total MUFA and PUFA and a lower SI compared to controls [45]. Our data show that in Stage 0-I, II and III-IV both C16:0 and C18:0 are significantly higher than in HD, while C18:1 increases in stages II and III-IV (Figure 2E). The increase of C18:1 typically correlates with the metastatic potential [46], as increased membrane fluidity is a key physical property determining adhesion and migration of tumor cells. The higher abundance of lauric (C12:0) and oleic acids we measured in stage III-IV CD81sEV may be explained by the accelerated metabolism of advanced cancer [47].

Proteomics of CD81sEV identified 899 proteins, 97% of which were comprehensive of all vesicles and 95% specific for exosomes and 81% of the top 100 Vesiclepedia proteins were detected in our dataset, while 83% were common to Exocarta, supporting the efficiency of our CD81-capture. The integral membrane protein 2B (ITMB2) is involved in p53-independent apoptotis and has been identified in stage 0-I [48]. Palmitoyl-protein thioesterase 1 (PPT1), also identified in stage 0-I, is increased in cancer and associated with poor survival [49]. This indicates that even in very early melanoma relevant changes in protein composition of circulating CD81sEV may occur, justifying the rare cases of metastatisation [50]. Insulin-like growth factor-binding protein 5 (IGFBP5) and Syntenin-1 were identified in stage II CD81sEV. The presence of IGFBP5, a tumor suppressor [51], in circulating sEV suggests its discharge from cells, likely favouring tumour progression. Syntenin can support tumor cell proliferation and migration [52] and its presence in sEV could mediate tumor progression. When we quantified the proteins detected by mass spectrometry by label free approach five proteins were significantly and differentially expressed in CD81sEV. APOA5, PON1, PON3, CD14 were increased in stage II, an interesting finding since stage II is at borderline between tumor *in situ* (stage 0-I) and distant metastasis (stage III-IV). APOA5, expressed by platelet-derived EV (ExoCarta) and podocyte-specific CR1-immunocaptured urine exosomes, modulates intra/extracellular triacylglycerol metabolism [53, 54] and this may relate to the differences measured in FA composition. PON1, is implicated in eliminating carcinogenic lipid-soluble radicals. In esophageal squamous cell carcinoma increased oxidative stress is associated with decreased antioxidant PON1 activities [55]. PON1 levels may act as indicator of oxidative stress in cancer [56]. PON3, overexpressed in tumors, promotes cell death resistance. Moreover, PON3 can impair ER stress-induced apoptotic MAPK signalling [57]. Of note, APOA5, PON1 and PON3 displayed a direct interaction in STRING analysis. PON1 and PON3 are involved in the lipoxygenase pathway (Figure 4C), leading to the generation of eicosanoids impacting cancer development, progression and immune responses [58]. Finally, of the four proteins increased in stage II CD81sEV, CD14 monocyte marker displayed the highest expression. Myeloid cell alterations including the accumulation of myeloid-derived suppressor cells, are typical in advanced stages [59]. However, routinely performed blood counts have evidenced survival associated alterations of peripheral blood leukocytes, including an increase in monocytes, also in early-stage melanoma patients [60]. In stage III-IV CD81sEV we found a decrease of Rap1b compared to HD. This was surprising since Rap1b is involved in MAPK and integrin activation in melanoma, [61], but was also identified as pan-EV marker [62]. Furthermore, Rap1b is expressed by platelet-derived sEV, thus physiologically present in circulating EV [62]. The decrease we measured in CD81sEV may thus potentially depend on the expansion of other EV populations, for instance deriving from immunosuppressive immune cells accumulating during progression.

The alteration of specific proteins and FA in CD81sEV of early-stage disease, especially stage II, may be of clinical significance. Indeed, stage II patients may have a worse melanoma-related survival compared to advanced patients [63]. Future research, combining the study of multiple biologic macromolecules in circulating EV, such as lipids, proteins, nucleic acids and carbohydrates, could be useful in terms of diagnosis, treatment and follow up of cancer patients.

5. Conclusions

Our results could contribute to intercept those patients who remain at high risk of relapse and thus may benefit from adjuvant therapy, currently intended only for stage III patients. Considering that liquid biopsy prognostic markers are usually searched for in stage III-IV patients while earlier stages are only beginning to be unveiled, stresses the importance of our findings [63, 64].
We propose that the combined investigation of FA and protein alterations in plasma CD81sEV could represent a new and useful approach to improve the diagnosis and treatment of cutaneous melanoma, especially in early stages.

Supplementary Materials: The following are available online at www.mdpi.com/xxx/s1,

Table S1. Clinicopathological features of melanoma patients

Figure S1: Fatty acids in total sEV

Figure S2: Proteomic analysis of CD81sEV

Author Contributions:

Writing-original draft preparation and data curation, **GP and VH**; Data collection and analyses, methodology, **SC, MC, AM, LB, FI, EM, SCe, IR, FC, CR and ADB**; Resources and conceptualization, **SCa** and **SRM**; Conceptualization, supervision and writing-reviewing and editing, **LL** and **CF**.

Funding:

This research was funded by Associazione Italiana per la Ricerca sul Cancro (AIRC) (IG25078 to VH) and was supported by the Current Research Funding and WFR GR-2011-02351400 provided to LL from the Italian Ministry of Health and by Fondi 5x1000 Ministero della Salute 2015 (D/17/1VH to VH).

Institutional Review Board Statement:

The study was conducted according to the guidelines of the Declaration of Helsinki, and approved by the Ethical Committee of Azienda Policlinico Umberto I, University Sapienza, Rome, Italy (Board resolution approval number #35/2017) .

Informed Consent Statement:

Informed consent was obtained from all subjects involved in the study.

Data Availability Statement:

Proteomic data are deposited in Proteome Xchange database with identifier PXD024434.

Acknowledgments:

We acknowledge for participating in the initial phase of data collection Paola Corsetti, Diego Abbenante, Emanuele Crincoli and Antonio Giovanni Richetta of Sapienza University of Rome, Italy.

Conflicts of Interest:

The authors declare no conflict of interest. The funders had no role in the design of the study; in the collection, analyses, or interpretation of data; in the writing of the manuscript, or in the decision to publish the results.

References

1. Ludwig N, Whiteside TL, Reichert TE. Challenges in Exosome Isolation and Analysis in Health and Disease. *Int J Mol Sci*. 2019;20:4684
2. van Niel G, D'Angelo G, Raposo G. Shedding light on the cell biology of extracellular vesicles. *Nat Rev Mol Cell Biol*. 2018;19:213-228
3. Kalluri R. The biology and function of exosomes in cancer. *J Clin Invest*. 2016;26:1208-1215
4. Vinik Y, Ortega F.G, Mills G.B, Lu Y, Jurkowicz M, Halperin S, Aharoni M, Gutman M, Lev S. Proteomic analysis of circulating extracellular vesicles identifies potential markers of breast cancer progression, recurrence, and response. *Sci Adv.* 2020;6:eaba5714
5. Mo Z, Cheong JYA, Xiang L, Le MTN, Grimson A, Zhang DX. Extracellular vesicle-associated organotropic metastasis. *Cell Prolif.* 2021;54:e12948
6. Xiao D, Barry S, Kmetz D, Egger M, Pan J, Rai SN, Qu J, McMasters KM, Hao H. Melanoma cell-derived exosomes promote epithelial-mesenchymal transition in primary melanocytes through paracrine/autocrine signaling in the tumor microenvironment. *Cancer Lett.* 2016;376:318-27
7. Alegre E, Zubiri L, Perez-Gracia JL, González-Cao M, Soria L, Martín-Algarra S, González A. Circulating melanoma exosomes as diagnostic and prognosis biomarkers. *Clin Chim Acta*. 2016;454:28-32
8. Logozzi M, De Milito A, Lugini L, Borghi M, Calabrò L, Spada M, Perdicchio M, Marino ML, Federici C, et al. High levels of exosomes expressing CD63 and caveolin-1 in plasma of melanoma patients. *PLoS One*. 2009;4:e5219
9. Aubuchon MM, Bolt LJ, Janssen Heijnen ML, Verleisdonk Bolhaar ST, van Marion A, van Berlo CL. Epidemiology, management and survival outcomes of primary cutaneous melanoma: a ten-year overview. *Acta Chir Belg*. 2016;117:29-35
10. Boutros C, Tarhini A, Routier E, Lambotte O, Ladurie FL, Carbonnel F, Izzeddine H, Marabelle A, Champiat S, et al. Safety profiles of anti-CTLA-4 and anti-PD-1 antibodies alone and in combination. *Nat Rev Clin Oncol*. 2016;13:473-486
11. Lugini L, Matarrese P, Tinari A, Lozupone F, Federici C, Iessi E, Gentile M, Luciani F, Parmiani G, et al. Cannibalism of live lymphocytes by human metastatic but not primary melanoma cells. *Cancer Res*. 2006;66:3629-3638
12. Tyrell R, Antia C, Stanley S, Deutsch GB. Surgical resection of metastatic melanoma in the era of immunotherapy and targeted therapy. *Melanoma Manag.* 2017;4:61-68
13. Morton DL, Davtyan DG, Wanek LA, Foshag LJ, Cochran AJ. Multivariate analysis of the relationship between survival and the microstage of primary melanoma by Clark level and Breslow thickness. *Cancer*.1993;71:3737-3743
14. De Giorgi V, Pinzani P, Salvianti F, Panelos J, Paglierani M, Janowska A, Grazzini M, Wechsler J, Orlando C et al. Application of a filtration- and isolation-by-size technique for the detection of circulating tumor cells in cutaneous melanoma. *J Invest Dermatol*. 2010;130:2440-2447
15. Ardekani GS, Jafarnejad SM, Khosravi S, Martinka M, Ho V, Li G. Disease progression and patient survival are significantly influenced by BRAF protein expression in primary melanoma. *Br J Dermatol*. 2013;169:320-328
16. Díaz-Lagares A, Alegre E, Arroyo A, González-Cao M, Zudaire ME, Viteri S, Martín-Algarra S, González A. Evaluation of multiple serum markers in advanced melanoma. *Tumour Biol*. 2011;32:1155-1161
17. Khoja L, Shenjere P, Hodgson C, Hodgetts J, Clack G, Hughes A, Lorigan P, Dive C, Prevalence and heterogeneity of circulating tumour cells in metastatic cutaneous melanoma. *Melanoma Res*. 2014;24:40-46
18. Chen G, Huang A.C, Zhang W, Zhang G, Wu M, Xu W, Yu Z, Yang J, Wang B et al. Exosomal PD-L1 contributes to immunosuppression and is associated with anti-PD-1 response. *Nature*. 2018;560:382-386
19. Skotland T, Sandvig K, Llorente A. Lipids in exosomes: Current knowledge and the way forward (Open Access). *Progr Lipid Res.* 2017;66:30-41
20. Skotland T, Hessvik NP, Sandvig K, Llorente A. Exosomal lipid composition and the role of ether lipids and phosphoinositides in exosome biology. *J Lipid Res*. 2019;60:9-18
21. Record M, Carayon K, Poirot M, Silvente-Poirot S. Exosomes as new vesicular lipid transporters involved in cell-cell communication and various pathophysiologies. *Biochim Biophys Acta.* 2014;1841:108-120
22. Suming C, Amrita DC, Pragney D, Dickens A, Dastgheyb R, Bhargava P, Bi H, and Haughey NJ. Lipidomic characterization of extracellular vesicles in human serum. *J Circ Biomark*. 2019;8:1849454419879848
23. Federici C, Shahaj E, Cecchetti S, Camerini S, Casella M, Iessi E, Camisaschi C, Paolino G, Calvieri S et al. Natural-Killer-Derived Extracellular Vesicles: Immune Sensors and Interactors. *Front Immunol*. 2020;11:262
24. Shively S and Miller WR. The use of HMDS (hexamethyldisilazane) to Replace Critical Point Drying (CPD) in the Preparation of Tardigrades for SEM (Scanning Electron Microscope) Imaging. *Trans Kan Acad Sci*. 2009;112:198-200
25. Ichihara K and Fukubayashi Y. Preparation of fatty acid methyl esters for gas-liquid chromatography. *J Lipid Res*. 2010;51:635-640
26. Lalle M, Camerini S, Cecchetti S, Sayadi A, Crescenzi M, Pozio E. Interaction network of the 14-3-3 protein in the ancient protozoan parasite giardia duodenalis. *J Proteome Res*. 2012; 11:2666-2683
27. Keerthikumar S, Chisanga D, Ariyaratne D, Al Saffar H, Anand S, Zhao K, Samuel M, Pathan M, Jois M, et al. ExoCarta: A web-based compendium of exosomal cargo. *J Mol Biol.* 2016;428:688-692

28. Pathan M, Keerthikumar S, Chisanga D, Alessandro R, Ang CS, Askenase P, Batagov AO, Benito-Martin A, Camussi G, et al. A novel community driven software for functional enrichment analysis of extracellular vesicles data. *J Extracell Vesicles.* 2017; 6:1321455
29. Pathan M, Keerthikumar S, Ang CS, Gangoda L, Quek CY, Williamson NA, Mouradov D, Sieber OM, Simpson RJ, et al. FunRich: An open access standalone functional enrichment and interaction network analysis tool. *Proteomics*. 2015;15:2597-2601
30. Szklarczyk D, Gable AL, Lyon D, Junge A, Wyder S, Huerta-Cepas J, Simonovic M, Doncheva NT, Morris JH, et al. STRING v11: protein-protein association networks with increased coverage, supporting functional discovery in genome-wide experimental datasets. *Nucleic Acids Res*. 2019;47(D1):D607-D613
31. Perez-Riverol Y, Csordas A, Bai J, Bernal-Llinares M, Hewapathirana S, Kundu DJ, Inuganti A, Griss J, Mayer G, Eisenacher M, et al. The PRIDE database and related tools and resources in 2019: improving support for quantification data. *Nucleic Acids Res*. 2019;47(D1):D442-D450
32. Zhang X, Smits A, van Tilburg G, Ovaa H, Huber W, Vermeulen M. Proteome-wide identification of ubiquitin interactions using UbIA-MS. *Nat Protocols.* 2018;13:530-550
33. Huber W, Carey VJ, Gentleman R, Anders S, Carlson M, Carvalho BS, Bravo HC, Davis S, Gatto L et al. Orchestrating high-throughput genomic analysis with Bioconductor. *Nat Methods.* 2015;12:115-121
34. Ritchie ME, Phipson B, Wu D, Hu Y, Law CW, Shi W, Smyth GK. limma powers differential expression analyses for RNA-sequencing and microarray studies. *Nucleic Acids Res.* 2015;43:e47
35. Strimmer K. A unified approach to false discovery rate estimation. *BMC Bioinformatics*. 2008;9:303
36. Aclimandos WA, Heinemann D, Kelly SB, Sheraidah GA, Hungerford JL. Erythrocyte stearic to oleic acid ratio in patients with ocular melanoma. *Eye (Lond).* 1992;6:416-419
37. Matthews NH, Li WQ, Qureshi AA, Weinstock MA, Cho E. Epidemiology of Melanoma. *Cutaneous Melanoma: Etiology and Therapy*. Ward WH, Farma JM, editors. Brisbane (AU); 2017
38. Pietrowska M, Zebrowska A, Gawin M, Marczak L, Sharma P, Mondal S, Mika J, Polańska J, Ferrone S, et al. Proteomic profile of melanoma cell-derived small extracellular vesicles in patients' plasma: a potential correlate of melanoma progression. *J Extracell Vesicles*. 2021;10:e12063
39. Currie E, Schulze A, Zechner R, Walther TC, Farese RV Jr. Cellular fatty acid metabolism and cancer. *Cell Metab*. 2013;18:153-161
40. König L, Kasimir-Bauer S, Bittner AK, Hoffmann O, Wagner B, Santos Manvailer LF, Kimmig R, Horn PA, Rebman V. Elevated levels of extracellular vesicles are associated with therapy failure and disease progression in breast cancer patients undergoing neoadjuvant chemotherapy. *Oncoimmunology*. 2018;7:1 e137615
41. Tominaga N, Kosaka N, Ono M, Katsuda T, Yoshioka Y, Tamura K, Lötvall J, Nakagama H, Ochiya T. Brain metastatic cancer cells release microRNA-181c-containing extracellular vesicles capable of destructing blood–brain barrier. *Nat Commun.*2015;6:6716
42. Karimi N, Cvjetkovic A, Chul Jang S, Crescitelli R, Hosseinpour Feizi MA, Nieuwland R, Lötvall J, Lässer C. Detailed analysis of the plasma extracellular vesicle proteome after separation from lipoproteins. *Cell Mol Life Sci*. 2018;75:2873-2886
43. Sun Y, Saito K, Saito Y. Lipid Profile Characterization and Lipoprotein Comparison of Extracellular Vesicles from Human Plasma and Serum. *Metabolites.* 2019;9:259
44. Pandey M, Sharma LB, Singh S, Shukla VK. Erythrocyte membrane fatty acid profile and saturation index in gallbladder carcinogenesis: a case-control study. *World J Surg Oncol*. 2003;1:5
45. Amézaga J, Arranz S, Urruticoechea A, Ugartemendia G, Larraioz A, Louka M, Uriarte M, Ferreri C, Tueros I. Altered Red Blood Cell Membrane Fatty Acid Profile in Cancer Patients. *Nutrients*. 2018;10:1853
46. Chen M and Huang J. The expanded role of fatty acid metabolism in cancer: new aspects and targets. *Precis Clin Med*. 2019;2:183-191
47. Hashimoto M and Hossain S. Fatty Acids: from membrane ingredients to signaling molecules. *Biochemistry and Health Benefits of Fatty Acids.* 2018
48. Fleischer A and Rebollo A. Induction of p53-independent apoptosis by the BH3-only protein ITM2Bs. *FEBS Lett*. 2004;557:283-287
49. Rebecca VW, Nicastri MC, Fennelly C, Chude CI, Barber-Rotenberg JS, Ronghe A, McAfee Q, McLaughlin NP, Zhang G, et al. PPT1 Promotes Tumor Growth and Is the Molecular Target of Chloroquine Derivatives in Cancer. *Cancer Discov*. 2019;9:220-229
50. Richetta AG, Bottoni U, Paolino G, Clerico R, Cantisani C, Ambrifi M, Corsetti P, Calvieri S. Thin melanoma and late recurrences: it is never too thin and never too late. *Med Oncol*. 2014;31:909
51. Wang J, Ding N, Li Y, Cheng H, Wang D, Yang Q, Deng Y, Yang Y, Li Y, et al. Insulin-like growth factor binding protein 5 (IGFBP5) functions as a tumor suppressor in human melanoma cells. *Oncotarget*. 2015;6:20636-20649
52. Kashyap R, Roucourt B, Lembo F, Fares J, Carcavilla AM, Restouin A, Zimmermann P, Ghossoub R. Syntenin controls migration, growth, proliferation, and cell cycle progression in cancer cells. *Front Pharmacol*. 2015;6:241
53. Sharma B, Shukla P. Futuristic avenues of metabolic engineering techniques in bioremediation. *Biotechnol Appl Biochem*. 2020; [Epub ahead of print]
54. Prunotto M, Farina A, Lane L, Pernin A, Schifferli J, Hochstrasser DF, Lescuyer P, Moll S. Proteomic analysis of podocyte exosome-enriched fraction from normal human urine. *J Proteomics*. 2013;82:193-229

55. Sehitogulları A, Aslan M, Sayır F, Kahraman A, Demir H. Serum paraoxonase-1 enzyme activities and oxidative stress levels in patients with esophageal squamous cell carcinoma. *Redox Rep*. 2014;19:199-205
56. Malik UU, Siddiqui IA, Hashim Z, Zarina S. Measurement of serum paraoxonase activity and MDA concentrations in patients suffering with oral squamous cell carcinoma. *Clin Chim Acta*. 2014;430:38-42
57. Schweikert EM, Devarajan A, Witte I, Wilgenbus P, Amort J, Förstermann U, Shabazian A, Grijalva V, Shih DM, et al. PON3 is upregulated in cancer tissues and protects against mitochondrial superoxide-mediated cell death. *Cell Death Differ*. 2012;19:1549-1560
58. Pidgeon GP, Lysaght J, Krishnamoorthy S, Reynolds JV, O'Byrne K, Nie D, Honn KV. Lipoxygenase metabolism: roles in tumor progression and survival. *Cancer Metastasis Rev*. 2007;26:503-524
59. Huber V, Di Guardo L, Lalli L, Giardiello D, Cova A, Squarcina P, Frati P, Di Giacomo AM, Pilla L, et al. Back to simplicity: a four-marker blood cell score to quantify prognostically relevant myeloid cells in melanoma patients. *J Immunother Cancer*. 2021; 9(2): e001167.
60. Wagner NB, Luttermann F, Gassenmaier M, Forschner A, Leiter U, Garbe C, Eigentler TK. Absolute and relative differential blood count predicts survival of AJCC stage I-II melanoma patients scheduled for sentinel lymph node biopsy. *Australas J Dermatol*. 2020;61:e310-e318.
61. Gao L, Feng Y, Bowers R, Becker-Hapak M, Gardner J, Council L, Linette G, Zhao H, Cornelius LA. Ras-associated protein-1 regulates extracellular signal-regulated kinase activation and migration in melanoma cells: two processes important to melanoma tumorigenesis and metastasis. *Cancer Res*. 2006;66:7880-7888
62. Hoshino A, Kim HS, Bojmar L, Gyan KE, Cioffi M, Hernandez J, Zambirinis CP, Rodrigues G, Molina H, et al. Extracellular vesicle and particle biomarkers define multiple human cancers. *Cell*. 2020;182:1044-1061.
63. Poklepovic AS and Luke JJ. Considering adjuvant therapy for stage II melanoma. *Cancer*. 2020;126:1166-1174
64. Yushak M, Mehnert J, Luke J, Poklepovic A. Approaches to High-Risk Resected Stage II and III Melanoma. *Am Soc Clin Oncol Educ*. 2019;39:e207-e211